



1 **Intercomparison of four methods to estimate coral calcification under various**
2 **environmental conditions**

3 Miguel Gómez Batista¹, Marc Metian², François Oberhänsli², Simon Pouil², Peter W.
4 Swarzenski², Eric Tambutté³, Jean-Pierre Gattuso^{4,5}, Carlos M. Alonso Hernández¹, Frédéric
5 Gazeau⁴

6

7

8 ¹Centro de Estudios Ambientales de Cienfuegos, Cuba

9 ²International Atomic Energy Agency, Environment Laboratories, 4a Quai Antoine 1er, MC-
10 98000 Monaco, Principality of Monaco

11 ³Centre Scientifique de Monaco, Department of Marine Biology, MC-98000 Monaco,
12 Principality of Monaco

13 ⁴Sorbonne Université, CNRS, Laboratoire d'Océanographie de Villefranche, LOV, F-06230
14 Villefranche-sur-Mer, France

15 ⁵Institute for Sustainable Development and International Relations, Sciences Po, 27 rue Saint
16 Guillaume, F-75007 Paris, France

17

18 Correspondence to: Miguel Gómez Batista (mgomezbatista@gmail.com)

19

20 Keywords: Calcification; Coral; Alkalinity anomaly; Calcium anomaly; ⁴⁵Ca incorporation;

21 ¹³C incorporation



22 Abstract

23 Coral reefs are constructed by calcifiers that precipitate calcium carbonate to build
24 their shells or skeletons through the process of calcification. Accurately assessing coral
25 calcification rates is crucial to determine the health of these ecosystems and their response to
26 major environmental changes such as ocean warming and acidification. Several approaches
27 have been used to assess rates of coral calcification but there is a real need to compare these
28 approaches in order to ascertain that high quality and intercomparable results can be
29 produced. Here, we assessed four methods (total alkalinity anomaly, calcium anomaly, ^{45}Ca
30 incorporation and ^{13}C incorporation) to determine coral calcification of the reef-building coral
31 *Stylophora pistillata*. Given the importance of environmental conditions on this process, the
32 study was performed under two pH (ambient and low level) and two light (light and dark)
33 conditions. Under all conditions, calcification rates estimated using the alkalinity and calcium
34 anomaly techniques as well as ^{45}Ca incorporation were highly correlated. Such a strong
35 correlation between the alkalinity anomaly and ^{45}Ca incorporation techniques has not been
36 observed in previous studies and most probably results from improvements described in the
37 present paper. The only method which provided calcification rates significantly different from
38 the other three techniques was ^{13}C incorporation. Calcification rates based on this method
39 were consistently higher than those measured using the other techniques. Although reasons
40 for these discrepancies remain unclear, the use of this technique for assessing calcification
41 rates in corals is not recommended without further investigations.



42 1. Introduction

43 Calcification is the fundamental biological process by which organisms precipitate
44 calcium carbonate. Calcifying organisms take up calcium and carbonate or bicarbonate ions to
45 build their biomineral structures (aragonite, calcite and/or vaterite) which have physiological,
46 ecological and biogeochemical functions. Moreover, calcium carbonate plays a major role in
47 the services provided by ecosystems to human societies.

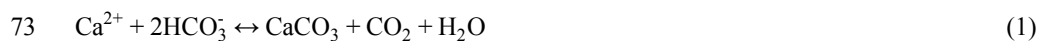
48 The ocean has absorbed large amounts of anthropogenic CO₂ since the start of the
49 industrial revolution and is currently sequestering about 22% of CO₂ emissions (average
50 2008-2017; Le Quéré et al., 2018). This massive input of CO₂ in the ocean impacts seawater
51 chemistry with a decrease in seawater pH, carbonate ion concentrations [CO₃²⁻] and an
52 increase in CO₂ and bicarbonate concentrations [HCO₃⁻]. These fundamental changes to the
53 carbonate system are referred to as “ocean acidification” (OA; Gattuso and Hansson, 2011).
54 Models project that the average surface water pH will drop by 0.06 to 0.32 pH units by the
55 end of the century (IPCC, 2014).

56 The effect of OA on the ocean is currently the subject of intense research with
57 particular attention to organisms producing CaCO₃. For instance, coral communities have
58 already proven to be particularly vulnerable to rapidly changing global environmental
59 conditions (e.g. Albright et al., 2018). In order to help project the future of coral reefs,
60 accurate estimates of calcification rates during realistic perturbation experiments are
61 necessary in order to produce high quality and intercomparable results (Langdon et al., 2010).

62 Several methods are available to quantify rates of coral calcification. Calcification can
63 be measured as the increase of CaCO₃ mass (e.g. the buoyant weight technique; Jokiel et al.,
64 1978) or following the incorporation of radio-labelled carbon or calcium in the skeleton



65 (Goreau, 1959), but also through the quantification of changes in a seawater constituent that is
66 stoichiometrically related to the amount of CaCO_3 precipitated. For instance, the alkalinity
67 anomaly technique (Smith and Key, 1975) has been widely used to estimate net calcification
68 of organisms and communities, especially of corals and coral reef environments (e.g. Smith
69 and Kinsey, 1978; Gazeau et al., 2015; Albright et al., 2016; Cyronak et al., 2018). Total
70 alkalinity (A_T) is directly influenced by bicarbonate and carbonate ion concentrations together
71 with a multitude of other minor compounds (Wolf-Gladrow et al., 2007). Calcification
72 consumes carbonate or bicarbonate, following the reversible reaction:



74 Calcification consumes two moles of HCO_3^- , hence decreasing A_T by two moles per
75 mole of CaCO_3 produced (eq. 1). It is possible to derive the rate of net calcification (gross
76 calcification - dissolution) by measuring A_T before and after incubating an organism or a
77 community. This method must assume, however, that only calcification influences A_T (Smith
78 and Key, 1975).

79 In contrast to A_T , the concentration of calcium (Ca^{2+}) in seawater is only biologically
80 influenced by net calcification and a 1:1 relationship can be used to derive net calcification
81 rates (eq. 1). The depletion of A_T and Ca^{2+} needs to be corrected for gains of A_T and Ca^{2+}
82 resulting from evaporation. These corrections can be applied through the incubation of
83 seawater in the absence of coral (Schoepf et al., 2017). Both the alkalinity anomaly and
84 calcium anomaly methods are non-destructive and typically show a solid agreement
85 (Chisholm and Gattuso, 1991; Murillo et al., 2014; Gazeau et al., 2015).

86 The ^{45}Ca incorporation technique has been used since the 1950's (Goreau and Bowen,
87 1955; Goreau, 1959). While earlier techniques showed low reproducibility, methodological
88 improvements led to a significant reduction of the deviations between replicates (see



89 Tambutté et al., 1995, for more details). The strength of this method is that it is extremely
90 sensitive for measuring short-term variations in gross calcification rates. However, in contrast
91 to the A_T and Ca^{2+} anomaly techniques, it is a sample-destructive method.

92 Previous studies designed to compare calcification rate estimates using the ^{45}Ca
93 incorporation and A_T anomaly methods revealed subtle discrepancies. For example, Smith and
94 Roth in Smith and Kinsey (1978) reported an overestimation of rates based on the ^{45}Ca
95 method. In contrast, Tambutté et al. (1995) and Cohen et al. (2017) reported a decrease in A_T
96 without concomitant incorporation of ^{45}Ca , therefore suggesting an overestimation of
97 calcification derived from A_T measurements. However, during these studies, in order to avoid
98 radioactive contamination of laboratory equipment, estimates of calcification were not
99 performed during the same incubations, but rather during incubations performed over two
100 consecutive days.

101 In contrast to the ^{45}Ca incorporation method, to the best of our knowledge, no studies
102 have used carbon-based incorporation techniques to estimate coral calcification rates in the
103 framework of ocean acidification. Past studies that compared carbon and calcium
104 incorporation rates in coral skeletons based on a double labelling technique with H^{14}CO_3 and
105 ^{45}Ca showed that only a minor proportion of the labelled seawater carbon is incorporated in
106 the skeleton (e.g. Marshall and Wright, 1998) and that the major source of dissolved inorganic
107 carbon for calcification is metabolic CO_2 (70–75% of the total CaCO_3 deposition; Furla et al.,
108 2000). Consequently, under both light and dark conditions, the rate of ^{45}Ca deposition appears
109 greater than the rate of ^{14}C incorporation (Furla et al., 2000). To the best of our knowledge,
110 only one study estimated calcification rates of a benthic calcifier (coralline algae) using a
111 stable carbon isotopic technique through addition of ^{13}C -labelled bicarbonate (McCoy et al.,
112 2016).



113 The present study aimed at comparing calcification rates measured using the alkalinity
114 and calcium anomaly methods, as well as the ^{45}Ca and ^{13}C incorporation techniques.



115 2. Material and Methods

116 Colonies of the reef-building coral *Stylophora pistillata* were incubated in the
117 laboratory, both in the light and dark, under ambient and lowered pH conditions. At ambient
118 pH (experiment conducted in July-August 2017), two sets of incubations were performed
119 using either ^{45}Ca or ^{13}C additions and calcification rates based on these techniques were
120 compared to those derived, during the same incubations, by the alkalinity and calcium
121 anomaly techniques. At lowered pH (experiment conducted in August 2018), no incubations
122 with ^{13}C addition were conducted and only the three other techniques were compared.

123 2.1. Biological material and experimental set-up

124 Specimens used in this experiment originated from colonies of the coral *Stylophora*
125 *pistillata* (Esper 1797) initially sampled in the Gulf of Aqaba (Red Sea, Jordan) and
126 transferred to the Scientific Centre of Monaco where they were cultivated under controlled
127 conditions for several years. In June 2017, terminal branches of *S. pistillata*, free of boring
128 organisms, were cut and suspended with a nylon line to allow tissues to fully cover the
129 exposed skeleton for at least five weeks (Tambutté et al., 1995; Houlbrèque et al., 2015). The
130 nubbins were fed with rotifers (once a day) and artemia nauplii (twice a week) and kept under
131 an irradiance of $200 \mu\text{mol photons m}^{-2} \text{s}^{-1}$ (12:12 light:dark photoperiod, light banks: HQI
132 250W Nepturion - BLV (Germany) / $200 \mu\text{mol photons m}^{-2} \text{s}^{-1}$), a seawater temperature of 25
133 ± 0.5 °C and a salinity of 38 ± 0.5 . Before the start of the experiment, specimens were
134 transferred to the International Atomic Energy Agency (IAEA). For the second set of
135 experiments in 2018, nubbins were prepared in June 2018 and cultured, under the conditions
136 described above, at IAEA except that colonies were fed twice a week with newly hatched



137 brine shrimp nauplii (1 nauplius ml⁻¹). Biometrics parameters (size, weight) on the biological
138 material are shown in Table 1.

139 Different types of incubations were conducted. In July-August 2017, one set of
140 incubations was performed under ambient pH conditions with the addition of radioactive
141 calcium dichloride (⁴⁵CaCl₂). During the same period, another set of incubations was
142 performed, under ambient pH conditions, with addition of labelled ¹³C-sodium bicarbonate
143 (¹³C-NaHCO₃ 99%). Finally, in August 2018, one set of incubations was performed under
144 lowered pH conditions (see thereafter for more details) with the addition of ⁴⁵CaCl₂. For all
145 sets of incubations, organisms were incubated for 5 to 11 hours (Table 1), both in the light
146 and dark, in 500 mL polyethylene beakers equipped with a magnetic stirrer (Fig. 1). Six and
147 five replicates were used, respectively, at ambient a low pH. Furthermore, for all sets of
148 incubations, one beaker was incubated, under the same conditions as the other beakers,
149 without coral and served as a control.

150 For each set of incubations, 2.4 L of seawater, pumped continuous from offshore of
151 the IAEA Monaco premises at 50 m depth, were filtered onto 0.2 µm (GF/F, 47 mm). For
152 incubations performed at lowered pH condition, pure CO₂ was bubbled in the 2.4 L initial
153 seawater batch using an automated pH-stat system (IKS Aquastar©) until the target pH was
154 reached. The pH electrode from the pH-stat system was inter-calibrated using a glass
155 combination electrode (Metrohm, Ecotrode Plus) calibrated on the total scale using a TRIS
156 buffer solution with a salinity of 35 (provided by A. Dickson, Scripps Institution of
157 Oceanography, San Diego). Initial pH_T (total scale) levels were set to ~7.2. It must be stressed
158 that pH levels were not regulated during the incubations. For ⁴⁵Ca-incubations, this initial
159 batch was spiked with ca. 10 µL of ⁴⁵CaCl₂ to reach a nominal activity of 25 Bq mL⁻¹. Before
160 distributing seawater to the experimental beakers, a one-milliliter aliquot of seawater was



161 removed for the precise determination of the initial activity. Samples were stored, in the dark,
162 in high-performance glass vials for 24 h before counting. For ^{13}C -incubations, to determine
163 seawater background isotopic level ($\delta^{13}\text{C}$) of the dissolved inorganic carbon pool ($\delta^{13}\text{C}-C_T$),
164 three 27 mL samples were collected and gently transferred to glass vials avoiding bubbles.
165 Then, ~ 8.95 mg of $^{13}\text{C}-\text{NaHCO}_3$ were added to the batch of filtered ambient seawater to
166 increase $\delta^{13}\text{C}-C_T$ to ca. 1,500‰. For the determination of $\delta^{13}\text{C}-C_T$ after enrichment, two 27
167 mL samples were handled as described above. The vials were then sealed after being
168 poisoned with 10 μL of saturated mercuric chloride (HgCl_2) and stored upside-down at room
169 temperature in the dark for subsequent analysis.

170 For all sets of incubations, samples for the measurements of pH_T , A_T (200 mL), and
171 Ca^{2+} concentrations (50 mL) were taken before distributing seawater to the experimental
172 beakers. While pH_T was measured immediately after sampling, samples for A_T measurements
173 were poisoned with 40 μL of 50% saturated HgCl_2 and stored in the dark at 4 °C pending
174 analysis less than two weeks later. Samples for $[\text{Ca}^{2+}]$ measurements were not poisoned and
175 stored in the dark at 4 °C pending analysis less than two weeks after sampling.

176 Gravimetrically determined amounts of filtered seawater (ca. 300 g) were transferred
177 to the incubation containers which were placed in a temperature-controlled (IKS Aquastar©)
178 water bath maintained at 25 ± 0.5 °C. Coral nubbins were suspended with a nylon line in the
179 experimental beakers 4 cm below the water level covered with transparent film to limit
180 evaporation (Fig. 1). During the low pH incubations conducted in 2018, to avoid a
181 physiological stress, coral nubbins were acclimated by gradually lowering pH to the target
182 levels during 24 h. This acclimation was performed in an open-flow 20 L aquarium (one full
183 water renewal per hour) using a pH-stat system as previously described and with a pH
184 decrease of ca. 0.03 units h^{-1} .



185 Incubations in the light were performed at an irradiance of $200 \mu\text{mol photons m}^{-2} \text{s}^{-1}$
186 during daytime whereas dark incubations were conducted at night. Before the beginning of
187 the incubations, all beakers (containing corals) were precisely weighed at $\pm 0.01 \text{ g}$ (Sartorius
188 BP 310S).

189 At the conclusion of the incubations, all beakers were precisely weighed to evaluate
190 evaporation and seawater samples were analyzed for pH_T , A_T and $[\text{Ca}^{2+}]$ as well as for ^{45}Ca
191 activity or $\delta^{13}\text{C}-C_T$ depending on the type of incubations. pH_T was measured immediately and
192 samples for A_T and $[\text{Ca}^{2+}]$ determinations were filtered onto $0.2 \mu\text{m}$ (GF/F, $\text{Ø} 47 \text{ mm}$),
193 poisoned with saturated HgCl_2 (only for A_T) and stored in the dark at 4 °C pending analysis
194 (within two weeks). The corals were then removed from the beakers for the analysis of
195 incorporated ^{45}Ca or ^{13}C . Three additional corals which were not incubated were processed
196 for carbon isotopic composition of the previously accreted calcium carbonate (see section
197 “2.3. Computations and statistics”).

198 2.2. Analytical techniques

199 Immediately after sampling, pH_T was measured on a Metrohm 826 mobile pH-logger
200 and a glass electrode (Metrohm, Ecotrode Plus) calibrated on the total scale using a TRIS
201 buffer of salinity 35 (provided by A. Dickson, Scripps University, USA). A_T was determined
202 in triplicate 50 mL subsamples by potentiometric titration on a titrator Titrand 888
203 (Metrohm) coupled to a glass electrode (Metrohm, Ecotrode Plus) and a thermometer
204 (pt1000). The pH electrode was calibrated before every set of measurements on the total scale
205 using a TRIS buffer of salinity 35 (provided by A. Dickson, Scripps University, USA).
206 Measurements were carried out at a constant temperature of 25 °C and A_T was calculated as
207 described in Dickson et al. (2007). Certified reference material (CRM; batches 143 and 156)



208 provided by A. Dickson (Scripps University, USA) were used to check precision (standard
209 deviation within measurements of the same batch) and accuracy (deviation from the certified
210 nominal value). Over the six series of A_T measurements performed during the experiment,
211 mean accuracy and precision (\pm SD) were respectively 7.2 ± 1.2 and $1.2 \pm 0.2 \mu\text{mol kg}^{-1}$.
212 $[\text{Ca}^{2+}]$ was determined in triplicate using the ethylene glycol tetra acetic acid (EGTA)
213 potentiometric titration (Lebel and Poisson, 1976). About 10 g of sampled seawater and 10 g
214 of HgCl_2 solution (ca. 1 mmol L^{-1}) were accurately weighed out. Then, about 10 g of a
215 concentrated EGTA solution (ca. 10 mmol L^{-1} , also by weighing) was added to completely
216 complex Hg^{2+} and to complex nearly 95% of Ca^{2+} . After adding 10 mL of borate buffer
217 ($\text{pH}_{\text{NBS}} \sim 10$) to increase the pH of the solution, the remaining Ca^{2+} was titrated by a diluted
218 solution of EGTA (ca. 2 mmol L^{-1}) using a titrator (Titrand 888, Metrohm) coupled to an
219 amalgamated silver combined electrode (Metrohm Ag Titrode). Following Cao and Dai
220 (2011), the volume of EGTA necessary to titrate the remaining ca. 5% of Ca^{2+} were obtained
221 by manually fitting a polynomial function to the first derivative of the titration curve using the
222 function “loess” of the R software¹. The EGTA solution was calibrated prior to each
223 measurement series using International Association for the Physical Sciences of the Oceans
224 (IAPSO) standard seawater (salinity = 38.005). Mean $[\text{Ca}^{2+}]$ precision obtained using this
225 technique was $2.9 \mu\text{mol kg}^{-1}$ ($n = 40$), corresponding to a coefficient of variation (CV) of
226 0.026%.

227 To determine the specific activity in radio-labelled seawater, the 1 mL aliquots were
228 transferred to 20 mL glass scintillation vials and mixed in proportion 1:10 (v:v) with
229 scintillation liquid Ultima Gold™ XR. According to a method adapted from Tambutté et al.
230 (1995), at the end of incubation sampled nubbins were immersed for 30 min in beakers

¹The R Development Core Team, R.: A language and environment for statistical computing, 2018.



231 containing 300 mL of unlabelled seawater to achieve isotopic dilution of the ^{45}Ca contained in
232 the gastrovascular cavity. Constant water motion was provided in the efflux medium by
233 magnetic stirring bars. Tissues were then dissolved completely in 1 mol L^{-1} NaOH at $90 \text{ }^\circ\text{C}$
234 for 20 min. The skeleton was rinsed twice in 1 mL NaOH and twice in 5 mL in MilliQ water.
235 It was then dried for 72 h at $60 \text{ }^\circ\text{C}$, weighed (referred thereafter to as skeleton dry weight),
236 and dissolved in 12 N HCl. Three 200 μL aliquots from each skeleton dissolution were
237 transferred to 20 mL glass scintillation vials and mixed with 10 mL scintillation liquid Ultima
238 Gold TM XR. Radioactive samples were thoroughly mixed to homogenize the solution and
239 kept in the dark for 24 h before counting. The radioactivity of ^{45}Ca was counted using a Tri-
240 Carb 2900 Liquid Scintillation Counter. Counting time was adapted to obtain a propagated
241 counting error of less than 5% (maximal counting duration was 90 min). Radioactivity was
242 determined by comparison with standards of known activities and measurements were
243 corrected for counting efficiency and physical radioactive decay.

244 The analyses of seawater $\delta^{13}\text{C}-C_T$ as well as of the ^{13}C signature of coral calcified
245 tissues were performed at Leuven University. For $\delta^{13}\text{C}-C_T$ analyses, a helium headspace (5
246 mL) was created in the vials and samples were acidified with 2 mL of phosphoric acid
247 (H_3PO_4 , 99%). Samples were left to equilibrate overnight to transfer all C_T to gaseous CO_2 .
248 Samples were injected in the carrier gas stream of an EA-IRMS (Thermo EA1110 and Delta
249 V Advantage), and data were calibrated with NBS-19 and LSVEC standards (Gillikin and
250 Bouillon, 2007). Corals were treated following the same protocol as for ^{45}Ca incorporation
251 measurements and powdered. Triplicate subsamples of carbonate powder ($\sim 100 \mu\text{g}$) were
252 placed into gas-tight vials, flushed with helium, and converted into CO_2 with H_3PO_4 . After 24
253 h, subsamples of the released CO_2 were injected into the EA-IRMS system as described
254 above. Data were calibrated with NBS-19 and LSVEC. Carbon isotope data are expressed in



255 the delta notation (δ) relative to Vienna Pee Dee Belemnite (VPDB) standard and were
256 calculated as:

$$257 \quad R_{\text{sample}} = \frac{\delta^{13}\text{C}_{\text{sample}}}{1000 + 1} \cdot R_{\text{VPDB}} \quad (2)$$

258 2.3. Computations and statistics

259 The carbonate chemistry was assessed using pH_T and A_T and the R package seacarb².
260 Propagation of errors on computed parameters was performed using the new function “error”
261 of the package seacarb (Orr et al., 2018) on the R software, considering errors associated to
262 the estimation of A_T as well as errors on dissociation constants.

263 Estimates of coral calcification rates based on changes in A_T and $[\text{Ca}^{2+}]$ during
264 incubations were computed following equations (3) and (4), respectively. As shown in these
265 equations, initial levels of A_T and $[\text{Ca}^{2+}]$ are not necessary to compute calcification rates and
266 only final values in the incubations with corals and without corals (controls) were used:

$$267 \quad G_{\text{AT}} = -\frac{(A_{T2} - A_{T1}) - (A_{T2c} - A_{T1c})}{2t} \cdot \frac{W_w}{W_c} = -\frac{(A_{T2} - A_{T2c})}{2t} \cdot \frac{W_w}{W_c} \quad (3)$$

$$268 \quad G_{\text{Ca}} = -\frac{(Ca_2 - Ca_1) - (Ca_{2c} - Ca_{1c})}{t} \cdot \frac{W_w}{W_c} = -\frac{(Ca_2 - Ca_{2c})}{t} \cdot \frac{W_w}{W_c} \quad (4)$$

269 where A_{T1} and Ca_1 are A_T and Ca^{2+} concentrations at the start of the incubations (in $\mu\text{mol kg}^{-1}$),
270 A_{T2}/A_{T2c} and Ca_2/Ca_{2c} are A_T and Ca^{2+} concentrations at the end of the incubations,
271 respectively with and without corals, t is the incubation duration in h, W_w and W_c are
272 respectively the mass of seawater (average between initial and final weights) and the coral
273 skeleton dry weight (g; DW). G_{AT} and G_{Ca} are therefore expressed in $\mu\text{mol CaCO}_3 \text{ g DW}^{-1} \text{ h}^{-1}$.
274 Error propagation was used to estimate errors:

²seacarb: seawater carbonate chemistry with R. Gattuso, J.-P., J. M. Epitalon, H. Lavigne, J. C. Orr, B. Gentili, M. Hagens, A. Hofmann, A. Proye, K. Soetaert and J. Rae, 2018. <https://cran.r-project.org/package=seacarb>



$$275 \quad SE_{G_{AT}} = \frac{\sqrt{SE_{AT_2}^2 + SE_{AT_{2c}}^2}}{2t} \cdot \frac{W_w}{W_c} \quad (5)$$

$$276 \quad SE_{G_{Ca}} = \frac{\sqrt{SE_{Ca_2}^2 + SE_{Ca_{2c}}^2}}{t} \cdot \frac{W_w}{W_c} \quad (6)$$

277 Coral calcification rates based on ^{45}Ca incorporation were estimated using measured
278 seawater activity and activity recorded in the skeleton digest. Rates were then normalized per
279 g skeleton dry weight using the formula:

$$280 \quad G_{^{45}\text{Ca}} = \frac{\text{Activity}_{\text{sample}} \cdot \frac{\text{Ca}}{\text{Activity}_{\text{seawater}}}}{W_c \cdot t} \quad (7)$$

281 where $\text{Activity}_{\text{sample}}$ is the average of counts per minute (CPM) of three 200 μL
282 aliquots from the dissolved skeleton sample, $\text{Activity}_{\text{seawater}}$ is the total CPM in the 1 mL
283 seawater samples, Ca is the $[\text{Ca}^{2+}]$ measured in the corresponding samples (average between
284 initial and final values, $\mu\text{mol kg}^{-1}$) and further converted to $\mu\text{mol L}^{-1}$ considering a
285 temperature of 25 °C and a salinity of 38, W_c is the skeleton dry weight (in g) and t the
286 incubation duration (h). $G_{^{45}\text{Ca}}$ is therefore expressed in $\mu\text{mol CaCO}_3 \text{ g DW}^{-1} \text{ h}^{-1}$. The standard
287 errors for these calcification rate estimates were propagated based on standard errors
288 associated with the measurements of triplicate samples for both $\text{Activity}_{\text{sample}}$ and $[\text{Ca}^{2+}]$.

289 The precipitation of calcium carbonate minerals (G) during the incubation interval was
290 also estimated using measured $\delta^{13}\text{C}$ values and isotope mass balance calculations [eq. (8) and
291 (9) below]. The CO_2 released during phosphoric acid digestion is derived from two sources:
292 new coral CaCO_3 and previously accreted skeletal carbonate mineral. The new carbon
293 acquired in each measured nubbins ($\delta^{13}\text{C}_N$) was assumed to have the same carbon isotope
294 composition as the labelled seawater C_T (average between initial and final level, $\delta^{13}\text{C}-C_T \sim$



295 1,400-1,700‰). The previously accreted skeletal material was assumed to have a $\delta^{13}\text{C}$ value
296 equal to the measured value for the background sample ($\delta^{13}\text{C}_P$). The $\delta^{13}\text{C}$ value ($\delta^{13}\text{C}_M$),
297 representing the mixture of new calcified material and previously accreted carbonate mineral,
298 is then calculated the following mixing equation:

$$299 \quad \delta^{13}\text{C}_M = f_G \cdot \delta^{13}\text{C}_N + (1 - f_G) \cdot \delta^{13}\text{C}_P \quad (8)$$

300 where f_G is the fraction of the calcium carbonate mineral precipitated during the experiment,
301 and $\delta^{13}\text{C}_N$ and $\delta^{13}\text{C}_P$ are the carbon isotope compositions of the newly precipitated and
302 previously accreted calcium carbonate, respectively. Equation (8) was solved for f_G to
303 determine the calcium carbonate precipitated during the incubation using:

$$304 \quad G_{13\text{C}} = \frac{f_G}{t \cdot M_{\text{CaCO}_3}} \cdot 1e^6 \quad (9)$$

305 where M_{CaCO_3} is the molar mass of calcium carbonate (g mol^{-1}) and t is the incubation
306 duration in h. $G_{13\text{C}}$ are therefore expressed in $\mu\text{mol CaCO}_3 \text{ g DW}^{-1} \text{ h}^{-1}$. The standard errors for
307 these calcification rate estimates were calculated based on standard errors associated with the
308 triplicate measurements of $\delta^{13}\text{C}_P$ and $\delta^{13}\text{C}_N$.

309 Model-II linear regressions (Sokal and Rohlf, 1995) were used to compare net
310 calcification rates obtained with the different methods. All regressions were performed using
311 function “lmodel2” of the package lmodel2³ on the R software.

³lmodel2: Model II Regression, Legendre P. and J. Oksanen, 2018. <https://cran.r-project.org/package=lmodel2>



312 3. Results

313 Environmental conditions at the start of the different incubations are shown in Table 2.

314 All incubations performed under ambient pH_T (~ 8.05) were conducted under carbonate
315 chemistry favorable to calcification with saturation states with respect to aragonite (Ω_a) well
316 above 1 (average of 4.0 ± 0.1 over the four incubations). In contrast, during experiments at
317 low pH_T (initial $\text{pH}_T \sim 7.2$), seawater was corrosive with respect to aragonite ($\Omega_a \sim 0.75$).
318 However, as pH was not regulated during the incubations (see previous section), it increased,
319 at lowered pH, to an average of 7.75 ± 0.03 ($n = 5$) in dark conditions and to an average of
320 7.84 ± 0.03 in light conditions ($n = 5$). Evolution of pH in control beakers (final pH_T of 7.78
321 and 7.48; $n = 1$ for both in the light and in the dark, respectively) showed that the observed
322 increase in beakers with corals was due to the additive effects of biological control
323 (photosynthesis minus respiration and calcification) and exchanges at the interface in the
324 light, and mostly due to CO_2 exchange with air during the much longer incubations performed
325 in the dark. Assuming linear variations with time, the average conditions of the carbonate
326 chemistry in the lowered pH experiments were slightly favorable to aragonite production (Ω_a
327 $= 1.4 \pm 0.2$ in the dark, $n = 5$ and 1.6 ± 0.05 in the light, $n = 5$). Under ambient pH conditions
328 (both for ^{45}Ca and ^{13}C incubations), pH did not change during incubations in the light
329 (average final pH_T of 8.05 ± 0.03 , $n = 12$, data not shown) while it decreased in the dark, due
330 to respiration and calcification, to reach an average pH_T level of 7.62 ± 0.07 , $n = 12$, data not
331 shown). In control beakers under ambient pH, pH_T slightly increased in the light (8.09 , $n = 2$)
332 and did not change in the dark (8.05 , $n = 2$).

333 ^{45}Ca activities in seawater did not change during the incubations, reaching a final
334 activity of 16.1 ± 1.2 ($n = 12$) and 28.5 ± 0.6 ($n = 10$) Bq mL^{-1} under ambient and lowered pH



335 conditions, respectively (including both dark and light incubations, data not shown).
336 Furthermore, for all incubations, these values are similar to those measured in beakers without
337 corals (control, data not shown). Under ambient pH levels (no incubation at lowered pH),
338 seawater was enriched in ^{13}C ($\delta^{13}\text{C}-C_T$) from a background level of $0.26 \pm 0.05\text{‰}$ ($n = 3$) to
339 $1,740 \pm 4.7\text{‰}$ ($n = 2$) and $1,634 \pm 11\text{‰}$ ($n = 2$) in the light and dark, respectively. During
340 light condition incubations, $\delta^{13}\text{C}-C_T$ levels decreased to an average of $1,636 \pm 10\text{‰}$ ($n = 6$,
341 data not shown) while they decreased to an average of $1,466 \pm 24\text{‰}$ in dark conditions ($n = 6$,
342 data not shown). Incubations in control beakers (without corals) showed that the majority of
343 $\delta^{13}\text{C}-C_T$ loss for both types of incubations (light and dark) was due to ^{13}C incorporation by
344 corals with a minor effect of gas exchanges at the interface (data not shown).

345 Changes in A_T and $[\text{Ca}^{2+}]$ in beakers containing corals as compared to control beakers,
346 during all sets of incubations, are shown in Table 3. Both variables declined in all incubations
347 as a consequence of coral calcification. Changes in A_T during incubations in control beakers
348 (data not shown) were comprised between 0.1 and 1.1% of the initial level. Similar results
349 were observed for $[\text{Ca}^{2+}]$ with a relative change comprised between 0.05 and 1.15% of the
350 initial value. These minimal changes were corroborated with no measurable changes in
351 seawater weight between the start and the end of all incubations (data not shown), showing
352 that evaporation, if any, was minimal using our experimental set-up over the considered
353 incubation times. At ambient pH levels, decreases in A_T and $[\text{Ca}^{2+}]$ (average of -380 ± 97 and
354 $-194 \pm 51 \mu\text{mol kg}^{-1}$ for both parameters, respectively, $n = 24$ including both ^{45}Ca and ^{13}C
355 incubations) were roughly similar under light and dark conditions although coral specimen
356 used for dark incubations were ca. 166% heavier (skeleton dry weight, see Table 1).
357 Incubations performed under lowered pH levels showed much lower A_T and $[\text{Ca}^{2+}]$ net
358 consumption rates than under ambient pH levels. Under these pH conditions, an extremely



359 high A_T consumption rate was observed in one beaker (dark incubation, see Table 3) while no
360 changes in $[Ca^{2+}]$ was observed in a total of three beakers (see Table 3). These rates have
361 been considered as outliers and were not included in the following analyses.

362 ^{45}Ca activities in coral skeleton reached maximum levels under ambient pH and light
363 conditions (average of 87.5 ± 9.1 Bq, $n = 6$). Although seawater was more enriched in ^{45}Ca at
364 the lower pH levels (see above), ^{45}Ca activity in corals incubated under these conditions were
365 much lower with lowest values measured in the dark (average of 19.6 ± 9.1 Bq, $n = 5$). $\delta^{13}C$
366 levels measured in coral skeletons (-3.69 to 8.92%) showed significant enrichment as
367 compared to background levels ($-3.97 \pm 0.35\%$, $n = 9$).

368 Estimated rates of calcification using the different techniques are presented in Table
369 A1 and are compared in Figs. 2, 3 and 4 as well as in Table 4. Rates were higher in the light
370 than in the dark and much lower rates were estimated at lowered pH. The rates measured by
371 alkalinity anomaly (G_{AT}) and calcium anomaly (G_{Ca}) techniques were highly correlated (Fig.
372 2; $R^2 = 0.98$, $p < 0.01$, $n = 34$). No significant difference was observed between rates
373 measured by the two methods (see Table 4 for the 95% confidence intervals of the slope and
374 intercept). The ^{45}Ca method provided also very similar rates than the two previous approaches
375 (Fig. 3; G_{Ca} vs. $G_{^{45}Ca}$ not shown) although the slope and the intercept of the geometric
376 regression between G_{AT} and $G_{^{45}Ca}$ were significantly different from 1 and 0, respectively.
377 Finally, the only approach that did not provide similar rates to the others was the ^{13}C
378 incorporation technique. Calcification rates based on this method were systematically higher
379 than those measured using the other three techniques (see Table 4), and rates were not always
380 significantly related (e.g. $R^2 = 0.33$, $p > 0.05$, $n = 12$ for G_{AT} vs $G_{^{13}C}$, see Fig. 4; other
381 relationships not shown).



382 4. Discussion

383 Under all experimental conditions (ambient pH vs low pH, light vs dark), significant
384 consumption rates of A_T and Ca^{2+} as well as significant incorporation rates of ^{45}Ca and ^{13}C
385 were observed in the zooxanthellate coral *Stylophora pistillata*. For all methods, calcification
386 rates were lower in dark than in light conditions. Such trends are expected as it has long been
387 established that calcification rates increase in zooxanthellate corals during periods in which
388 photosynthesis is occurring (Yonge, 1931), a process known as light-enhanced calcification
389 (e.g. Gattuso et al., 1999). Even under lowered pH conditions, at pH levels far below those
390 predicted to occur in the next decades (starting pH_T of ca. 7.2, average pH_T during incubations
391 of ca. 7.5), all corals appeared to produce calcifying structures under both light and dark
392 conditions. The organisms selected for this experiment were fully coated with tissues with no
393 exposed calcareous structures which can explain the absence of observable net dissolution
394 such as reported by Cohen et al. (2017) in a similar study. Since our experimental protocol
395 was not designed to address the potential impact of decreasing pH levels on calcification rates
396 of this species (no control of carbonate chemistry during incubations, no acclimation of the
397 organisms etc.), we will not discuss further the observed decrease of calcification rates
398 identified by the three techniques used at these pH levels.

399 Under all experimental conditions, rates of calcification calculated using the alkalinity
400 and the calcium anomaly techniques were highly correlated with a slope of 1 and no
401 significant intercept. These results are consistent with previously published data on colonies
402 of *Pocillopora damicornis* (Chisholm and Gattuso, 1991), *Cladocora caespitosa* (Gazeau et
403 al., 2015) and several other coral species (Murillo et al. 2014). Although the precision
404 obtained on Ca^{2+} measurements is among the highest reported to date (Gazeau et al., 2015),



405 the alkalinity anomaly technique appears as the most appropriate to estimate calcification
406 rates of isolated corals (better precision, stronger signals). As observed by Murillo et al.
407 (2014), this is not true when an entire community including sediment is investigated. The
408 occurrence of several processes in the sediment that can impact A_T prevents the use of this
409 technique. It is therefore recommended to use the calcium anomaly technique when working
410 in natural settings, assuming that Ca^{2+} concentrations are measured with an analytical
411 technique as precise as the one used in our study ($\text{CV} < 0.05\%$). Similarly, although
412 corrections are possible when applying the alkalinity anomaly technique on organisms that
413 significantly release nutrients (echinoderms, bivalves etc.), the use of the calcium anomaly
414 technique is highly recommended instead (Gazeau et al., 2015).

415 Calcification rate estimates based on changes of A_T or Ca^{2+} were highly correlated
416 with estimates based on ^{45}Ca incorporation in corals. These results are not consistent to those
417 reported by Smith and Roth (in Smith and Kinsey, 1978), Tambutté et al. (1995) and Cohen et
418 al. (2017). These studies revealed discrepancies between the alkalinity anomaly and the ^{45}Ca
419 incorporation techniques. Smith and Roth found that rates measured with the ^{45}Ca method
420 were higher than those measured using the alkalinity anomaly technique (significant ^{45}Ca
421 incorporation at $\Delta A_T = 0$). Results from both Tambutté et al. (1995) and Cohen et al. (2017)
422 suggested the opposite with a decrease in A_T consumption without any concomitant ^{45}Ca
423 incorporation. A number of reasons may explain these discrepancies. First, the present study
424 is the first one comparing these techniques in the same incubations, in contrast to the other
425 ones in which incubations for A_T anomaly and ^{45}Ca incorporation were performed over two
426 consecutive days (due to radioactive contamination issues). Second, calcification expressed as
427 absolute changes in A_T during incubations, measured during our experiment, were at least one
428 order of magnitude higher than measured during these studies (44,200 to 745,600 nmol vs



429 less than 4,000 nmol in previous experiments). Cohen et al. (2017) have shown that such
430 discrepancies were much higher at very low rates and that the ratio between rates estimated
431 based on ^{45}Ca incorporation and A_T consumption were getting closer to 1 with increasing
432 calcification rates. Nevertheless, even at the highest levels of calcification computed during
433 these studies, ^{45}Ca -based rates were still significantly different from ΔA_T -based rates, which is
434 in contrast with our results.

435 As already mentioned, although calcification rates of the present study were lower at
436 lowered pH levels, there was still a close to perfect agreement between the different
437 techniques. While the ^{45}Ca labelling technique is thought to provide rates of gross
438 calcification, there is no doubt that both the A_T and Ca^{2+} anomaly techniques allow the
439 estimation of net calcification rates (gross calcification – dissolution). A full agreement of
440 rates computed from these methods further suggest that no dissolution of previously
441 precipitated CaCO_3 structures occurred during our study, even under lowered pH conditions.
442 The corals used in our experiment were fully covered with tissues which is likely the reason
443 that no dissolution was measured.

444 Furthermore, we must note that the protocol for ^{45}Ca incorporation considered in our
445 study differed from the one used in the above-mentioned past studies. A much smaller activity
446 was used ($0.025 \text{ kBq mL}^{-1}$) compared to Tambutté et al. (1995; 40 kBq mL^{-1}) and Cohen et al.
447 (2017; 9 kBq mL^{-1}). Moreover, in contrast to Cohen et al. (2017), rates were not corrected for
448 ^{45}Ca incorporation on the skeleton of dead corals. This choice was motivated by the absence
449 of detectable radioactivity on bare skeletons exposed for 7 h and treated with the same
450 protocol than one used in our study (Lanctôt, pers. comm.).

451 To the best of our knowledge, this is the first study comparing calcification rates
452 measured using the ^{13}C labelling technique to the more widely used alkalinity and calcium



453 anomaly techniques. It shows that ^{13}C -derived rates were systematically higher and much
454 more variable (with large uncertainties) than the ones estimated using the two other
455 techniques. As already mentioned, several studies have shown that most of the carbon
456 precipitated in the skeleton comes from coral and its symbiotic zooxanthellae (e.g. Erez,
457 1978; Furla et al., 2000), leading to an underestimation of calcification rates based on
458 labelled, radioactive carbon incorporation. As there is no reason for ^{13}C to behave differently,
459 our results appear inconsistent with a metabolic source of carbon. As the nubbins were treated
460 following the same protocol as for ^{45}Ca incorporation measurements, it is unclear why much
461 stronger ^{13}C incorporation were obtained and why variability is so high. Before better insights
462 on such discrepancies can be developed, we recommend to avoid this technique to estimate
463 coral calcification rates.

464 Although our study was designed to compare different techniques to estimate
465 calcification rates and not to define the best experimental approach to study the effects of
466 ocean acidification on coral species using these different approaches, our results provide some
467 insights that we further discuss in the following section. Measuring and comparing
468 calcification rates of organisms under varying pH conditions requires the careful choice of a
469 volume and a time interval such that the precision of the calcification rate measurement is
470 large enough to observe significant signals and that the change in carbonate chemistry
471 parameters between the beginning and end of the incubation is small compared to the range of
472 these parameters in the different treatments (Langdon et al. 2010).

473 Table 5 illustrates the incubation time necessary to obtain measurable changes
474 considering the ratio between incubation volume and coral size chosen for our study. As the
475 ^{13}C incorporation method did not provide reliable rates, this technique was not considered in
476 this analysis. The threshold for significant signals was set at 10-fold the analytical precision



477 of the instruments (Langdon et al. 2010) for A_T and Ca^{2+} measurements (1.2 and 2.9 $\mu\text{mol kg}^{-1}$,
478 respectively) and above the detection limit of 15 cpm for ^{45}Ca activity estimated. Maximum
479 incubation times have been determined considering a maximum decrease of C_T by 10%
480 (Langdon et al. 2010).

481 Under light and ambient pH conditions, even if the ratio between incubation volume
482 and nubbin size is much higher than for previous similar studies (e.g. Cohen et al. 2017), all
483 methods would allow a precise estimation of calcification rates over very short incubation
484 times (~15 min to 1 h, depending on the method) while leading to moderate changes in C_T (<
485 10%). In the dark, and at ambient pH conditions, in the absence of C_T increase by
486 photosynthesis, the increase of C_T due to respiration, of which only a minor portion is
487 compensated by calcification, narrows the possible incubation period to 12 h. However, this is
488 still much larger than the incubation time allowing to obtain a significant signal with the three
489 methods (~20 min to ~2 h). At lower pH, both under light and dark conditions, and using
490 open systems without a continuous pH regulation as in our study, it is obvious that the
491 calcium anomaly technique is not well adapted to this experimental protocol. Indeed, as a
492 consequence of lower calcification rates at lower pH and important CO_2 degassing, incubation
493 times necessary to obtain significant signals using this technique are too large to maintain the
494 carbonate parameters within an acceptable range ($\Delta C_T < 10\%$). This is not insurmountable as
495 a continuous regulation of pH using for instance pure CO_2 bubbling or incubations performed
496 in a closed container (i.e. without contact to the atmosphere) would alleviate these problems.
497 Nevertheless, if such experimental protocols cannot be followed, our results show that the
498 alkalinity anomaly and ^{45}Ca incorporation techniques are still sensitive enough, at lowered
499 pH, to estimate reliable calcification rates in zooxanthellate corals maintained in open-



500 systems without continuous pH regulation, while maintaining acceptable changes in the
501 carbonate chemistry.

502 In conclusion, the present study is the first one allowing a direct (i.e. during the same
503 incubations) comparison of three methods used to estimate coral calcification rates, the
504 calcium and alkalinity anomaly techniques and the ^{45}Ca incorporation technique. These
505 methods provided very consistent calcification rates of the coral *Stylophora pistillata*
506 independently of the conditions set for the incubations (light vs dark, ambient vs low pH).
507 Among these three methods, the alkalinity anomaly and the ^{45}Ca incorporation techniques
508 appear to be the most sensitive allowing the quantification of coral calcification rates without
509 significant changes in targeted environmental conditions. In contrast, the ^{13}C incorporation
510 technique did not provide reliable calcification rates and its use is not recommended until
511 further investigations clarify the discrepancies. Finally, this study was restricted to a single
512 coral species and used nubbins fully covered with tissues. Conducting similar comparison
513 studies with other coral species as well as other major calcifying groups widely studied in the
514 context of ocean acidification (e.g. coralline algae, molluscs etc...) would be necessary.



515 Acknowledgements

516 This work was supported by the IAEA's Ocean Acidification International Coordination
517 Center (OA-ICC) and the IAEA-ICTP Sandwich Training Educational Programme (STEP)
518 and Project "Strengthening the National System for Analysis of the Risks and Vulnerability of
519 Cuban Coastal Zone Through the Application of Nuclear and Isotopic Techniques" National
520 Program PNUOLU /4-1/ 2 No. /2017 of the National Nuclear Agency (AENTA). We thank
521 the Monaco government, the Centre Scientifique de Monaco for propagating and maintaining
522 the coral nubbins and Samir Alliouane for technical assistance for total alkalinity and calcium
523 measurements.



524 REFERENCES

- 525 Albright, R., Caldeira, L., Hosfelt, J., Kwiatkowski, L., Maclaren, J. K., Mason, B. M.,
526 Nebuchina, Y., Ninokawa, A., Pongratz, J., Ricke, K. L., Rivlin, T., Schneider, K.,
527 Sesboué, M., Shamberger, K., Silverman, J., Wolfe, K., Zhu, K., and Caldeira, K.:
528 Reversal of ocean acidification enhances net coral reef calcification, *Nature*, 531, 362,
529 10.1038/nature17155, 2016.
- 530 Albright, R., Takeshita, Y., Koweek, D. A., Ninokawa, A., Wolfe, K., Rivlin, T., Nebuchina,
531 Y., Young, J., and Caldeira, K.: Carbon dioxide addition to coral reef waters suppresses
532 net community calcification, *Nature*, 555, 516, 10.1038/nature25968, 2018.
- 533 Cao, Z., and Dai, M.: Shallow-depth CaCO₃ dissolution: Evidence from excess calcium in the
534 South China Sea and its export to the Pacific Ocean, *Global Biogeochemical Cycles*, 25,
535 doi:10.1029/2009GB003690, 2011.
- 536 Chisholm, J. R. M., and Gattuso, J.-P.: Validation of the alkalinity anomaly technique for
537 investigating calcification and photosynthesis in coral reef communities, *Limnology and*
538 *Oceanography*, 36, 1232-1239, 1991.
- 539 Cohen, S., Krueger, T., and Fine, M.: Measuring coral calcification under ocean acidification:
540 methodological considerations for the ⁴⁵Ca-uptake and total alkalinity anomaly
541 technique, *PeerJ*, 5, e3749, 10.7717/peerj.3749, 2017.
- 542 Cyronak, T., Andersson, A. J., Langdon, C., Albright, R., Bates, N. R., Caldeira, K., Carlton,
543 R., Corredor, J. E., Dunbar, R. B., Enochs, I., Erez, J., Eyre, B. D., Gattuso, J.-P.,
544 Gledhill, D., Kayanne, H., Kline, D. I., Koweek, D. A., Lantz, C., Lazar, B., Manzello,
545 D., McMahon, A., Meléndez, M., Page, H. N., Santos, I. R., Schulz, K. G., Shaw, E.,
546 Silverman, J., Suzuki, A., Teneva, L., Watanabe, A., and Yamamoto, S.: Taking the



- 547 metabolic pulse of the world's coral reefs, PLOS ONE, 13, e0190872,
548 10.1371/journal.pone.0190872, 2018.
- 549 Dickson, A. G., Sabine, C. L., and Christian, J. R.: Guide to best practices for ocean CO₂
550 measurements. PICES Special Publication 3, 191pp, 2007.
- 551 Erez, J.: Vital effect on stable-isotope composition seen in foraminifera and coral skeletons,
552 Nature, 273, 199-202, 10.1038/273199a0, 1978.
- 553 Furla, P., Galgani, I., Durand, I., and Allemand, D.: Sources and mechanisms of inorganic
554 carbon transport for coral calcification and photosynthesis, Journal of Experimental
555 Biology, 203, 3445-3457, 2000.
- 556 Gattuso, J.-P., and Hansson, L.: Ocean acidification: background and history, in: Ocean
557 acidification, edited by: Gattuso, J.-P., and Hansson, L., Oxford University Press,
558 Oxford, 1-20, 2011.
- 559 Gazeau, F., Urbini, L., Cox, T. E., Alliouane, S., and Gattuso, J. P.: Comparison of the
560 alkalinity and calcium anomaly techniques to estimate rates of net calcification, Marine
561 Ecology Progress Series, 527, 1-12, 2015.
- 562 Gillikin, D. P., and Bouillon, S.: Determination of $\delta^{18}\text{O}$ of water and $\delta^{13}\text{C}$ of dissolved
563 inorganic carbon using a simple modification of an elemental analyser-isotope ratio
564 mass spectrometer: an evaluation, Rapid Communications in Mass Spectrometry, 21,
565 1475-1478, doi:10.1002/rcm.2968, 2007.
- 566 Goreau, T. F.: The physiology of skeleton formation in corals. I. A method for measuring the
567 rate of calcium deposition by corals under different conditions, Biological Bulletin, 116,
568 59-75, 1959.
- 569 Goreau, T. F., and Bowen, V. T.: Calcium uptake by a coral, Science, 122, 1188-1189,
570 10.1126/science.122.3181.1188, 1955.



- 571 Houlbrèque, F., Reynaud, S., Godinot, C., Oberhänsli, F., Rodolfo-Metalpa, R., and Ferrier-
572 Pagès, C.: Ocean acidification reduces feeding rates in the scleractinian coral
573 *Stylophora pistillata*, *Limnology and Oceanography*, 60, 89-99, doi:10.1002/lno.10003,
574 2015.
- 575 IPCC: Climate Change 2014: Synthesis Report. Contribution of Working Groups I, II and III
576 to the Fifth Assessment Report of the Intergovernmental Panel on Climate Change,
577 edited by: Team, C. W., Pachauri, R. K., and Meyer, L. A., IPCC, Geneva, Switzerland,
578 151 pp., 2014.
- 579 Jokiel, P. L., Maragos, J. E., and Franzisket, L.: Coral growth: buoyant weight technique, in:
580 Coral reefs: research methods, edited by: Stoddart, D. R., and Johannes, R. E., Paris:
581 Unesco, 379-396, 1978.
- 582 Langdon, C., Gattuso, J.-P., and Andersson, A. J.: Measurements of calcification and
583 dissolution of benthic organisms and communities, in: Guide to Best Practices for
584 Ocean Acidification Research and Data Reporting, 213-234, 2010.
- 585 Le Quéré, C., Andrew, R. M., Friedlingstein, P., Sitch, S., Hauck, J., Pongratz, J., Pickers, P.
586 A., Korsbakken, J. I., Peters, G. P., Canadell, J. G., Arneeth, A., Arora, V. K., Barbero,
587 L., Bastos, A., Bopp, L., Chevallier, F., Chini, L. P., Ciais, P., Doney, S. C., Gkritzalis,
588 T., Goll, D. S., Harris, I., Haverd, V., Hoffman, F. M., Hoppema, M., Houghton, R. A.,
589 Hurtt, G., Ilyina, T., Jain, A. K., Johannessen, T., Jones, C. D., Kato, E., Keeling, R. F.,
590 Goldewijk, K. K., Landschützer, P., Lefèvre, N., Lienert, S., Liu, Z., Lombardozzi, D.,
591 Metzl, N., Munro, D. R., Nabel, J. E. M. S., Nakaoka, S. I., Neill, C., Olsen, A., Ono,
592 T., Patra, P., Peregon, A., Peters, W., Peylin, P., Pfeil, B., Pierrot, D., Poulter, B.,
593 Rehder, G., Resplandy, L., Robertson, E., Rocher, M., Rödenbeck, C., Schuster, U.,
594 Schwinger, J., Séférian, R., Skjelvan, I., Steinhoff, T., Sutton, A., Tans, P. P., Tian, H.,



- 595 Tilbrook, B., Tubiello, F. N., van der Laan-Luijkx, I. T., van der Werf, G. R., Viovy, N.,
596 Walker, A. P., Wiltshire, A. J., Wright, R., Zaehle, S., and Zheng, B.: Global Carbon
597 Budget 2018, *Earth Syst. Sci. Data*, 10, 2141-2194, 10.5194/essd-10-2141-2018, 2018.
- 598 Lebel, J., and Poisson, A.: Potentiometric determination of calcium and magnesium in
599 seawater, *Marine Chemistry*, 4, 321–332, doi:10.1016/0304-4203(76)90018-9, 1976.
- 600 Marshall, A. T., and Wright, A.: Coral calcification: autoradiography of a scleractinian coral
601 *Galaxea fascicularis* after incubation in ^{45}Ca and ^{14}C , *Coral Reefs*, 17, 37-47,
602 10.1007/s003380050092, 1998.
- 603 McCoy, S. J., Pfister, C. A., Olack, G., and Colman, A. S.: Diurnal and tidal patterns of
604 carbon uptake and calcification in geniculate inter-tidal coralline algae, *Marine*
605 *Ecology*, 37, 553-564, doi:10.1111/maec.12295, 2016.
- 606 Murillo, L. J. A., Jokiel, P. L., and Atkinson, M. J.: Alkalinity to calcium flux ratios for corals
607 and coral reef communities: variances between isolated and community conditions,
608 *PeerJ*, 2, e249, 10.7717/peerj.249, 2014.
- 609 Orr, J. C., Epitalon, J.-M., Dickson, A. G., and Gattuso, J.-P.: Routine uncertainty
610 propagation for the marine carbon dioxide system, *Marine Chemistry*, 207, 84-107,
611 <https://doi.org/10.1016/j.marchem.2018.10.006>, 2018.
- 612 Schoepf, V., Hu, X., Holcomb, M., Cai, W.-J., Li, Q., Wang, Y., Xu, H., Warner, M. E.,
613 Melman, T. F., Hoadley, K. D., Pettay, D. T., Matsui, Y., Baumann, J. H., and Grottoli,
614 A. G.: Coral calcification under environmental change: a direct comparison of the
615 alkalinity anomaly and buoyant weight techniques, *Coral Reefs*, 36, 13-25,
616 10.1007/s00338-016-1507-z, 2017.
- 617 Smith, S. V., and Key, G. S.: Carbon dioxide and metabolism in marine environments,
618 *Limnology and Oceanography*, 20, 493-495, 1975.



- 619 Smith, S. V., and Kinsey, D. W.: Calcification and organic carbon metabolism as indicated by
620 carbon dioxide, in: Coral reefs: Research methods, edited by: Stoddart, D. R., and
621 Johannes, R. E., Monogr. Oceanogr. Methodol. 5. UNESCO, 1978.
- 622 Sokal, R. R., and Rohlf, F. J.: Biometry, the principles and practice of statistics in biological
623 research, 3rd ed. W. H. Freeman, New York, 1995.
- 624 Tambutté, E., Allemand, D., Bourge, I., Gattuso, J.-P., and Jaubert, J.: An improved Ca⁴⁵
625 protocol for investigating physiological mechanisms in coral calcification, Marine
626 Biology, 122, 453-459, 10.1007/bf00350879, 1995.
- 627 Wolf-Gladrow, D. A., Zeebe, R. E., Klaas, C., Körtzinger, A., and Dickson, A. G.: Total
628 alkalinity: the explicit conservative expression and its application to biogeochemical
629 processes, Marine Chemistry, 106, 287-300, doi:10.1016/j.marchem.2007.01.006,
630 2007.



631 Table 1. Experimental details for the series of incubations of the coral *Stylophora pistillata* performed under ambient and low pH, and in
 632 the light and dark following ⁴⁵Ca or ¹³C labelling. The ratio $W_w:W_c$ corresponds to the ratio between seawater weight (g) and skeletal dry
 633 weight (g). Values represent mean ± standard deviation (SD); n is the number of true replicates considered for each experiment.

pH conditions	Ambient (n = 6)				Lowered (n = 5)	
	⁴⁵ Ca		¹³ C		⁴⁵ Ca	
Added label	Light	Dark	Light	Dark	Light	Dark
Light conditions						
Coral size (mm)	33.2 ± 1.5	44.7 ± 1.5	36.3 ± 2.2	50.2 ± 1.7	26.0 ± 1.6	28.9 ± 1.9
Coral Skeleton dry weight (g)	2.5 ± 0.5	3.8 ± 0.7	2.6 ± 0.5	4.7 ± 0.5	2.1 ± 0.2	2.8 ± 0.4
Ratio $W_w:W_c$	126.4 ± 25.6	81.9 ± 14.7	106.9 ± 24.5	67.8 ± 7.5	146.5 ± 14.3	110.0 ± 12.4
Incubation time (h)	8	8	9.12	9.12	5	11



634 Table 2. Environmental conditions at the start of incubations of the coral *Sylophora pistillata*. pH on the total scale (pH_T), partial pressure
 635 of CO₂ (pCO₂ in μatm), total alkalinity (A_T in μmol kg⁻¹), dissolved inorganic carbon (C_T in μmol kg⁻¹), saturation states with respect to
 636 aragonite (Ω_a) and calcite (Ω_c) as well as calcium concentrations ([Ca²⁺] in μmol kg⁻¹) are presented. Labelled seawater ⁴⁵Ca activity
 637 (Activity_{seawater} in Bq mL⁻¹) and the isotopic level, of the seawater dissolved inorganic carbon pool (δ¹³C-C_T in ‰) are
 638 also shown. Means ± standard deviation of analytical triplicates (duplicates for δ¹³C-C_T) are shown when available.

pH conditions Added label	Ambient				Lowered ⁴⁵ Ca	
	⁴⁵ Ca		¹³ C		Light	Dark
Light conditions	Light	Dark	Light	Dark	Light	Dark
pH _T	8.05	8.05	8.06	8.05	7.21	7.24
pCO ₂	427.6 ± 8.2	438.8 ± 8.5	425.6 ± 8.2	424.1 ± 8.2	3,727.2 ± 66.8	3,460.1 ± 62.1
A _T	2,556.0 ± 0.5	2,620.0 ± 0.7	2,615.2 ± 0.6	2,535.9 ± 1.8	2,558.4 ± 0.3	2,552.9 ± 2.4
C _T	2,206.4 ± 7.4	2,264.1 ± 7.6	2,252.9 ± 7.7	2,188.2 ± 7.6	2,597.1 ± 2.5	2,579.8 ± 3.5
Ω _a	3.9 ± 0.2	4.0 ± 0.2	4.1 ± 0.2	3.9 ± 0.2	0.7 ± 0.0	0.8 ± 0.0
Ω _c	5.9 ± 0.3	6.1 ± 0.3	6.2 ± 0.3	5.9 ± 0.3	1.1 ± 0.1	1.2 ± 0.1
[Ca ²⁺]	11,179.6 ± 0.0	11,164.0 ± 2.0	11,096.5 ± 13.4	11,098.5 ± 2.8	11,281.2 ± 5.5	11,277.6 ± 0.3
Activity _{seawater} δ ¹³ C-C _T	16.6	15.1	-	-	28.5	30.4
	-	-	1,740 ± 4.7	1,634 ± 11	-	-

639



640 Table 3. Changes in total alkalinity (A_T) and calcium concentrations ($[Ca^{2+}]$) during the different types of incubations as compared to
 641 control beakers: $\Delta A_T = A_{T2} - A_{T2c}$, $\Delta[Ca^{2+}] = Ca_2 - Ca_{2c}$, both expressed in $\mu\text{mol kg}^{-1}$. Standard errors (SE) have been calculated as
 642 $\sqrt{SE_{A_T}^2 + SE_{Ca_2}^2}$ and $\sqrt{SE_{Ca_2}^2 + SE_{Ca_{2c}}^2}$ for A_T and $[Ca^{2+}]$, respectively, where SE correspond to standard errors associated with the
 643 measurement of three analytical replicates per sample. ^{45}Ca activity (Activity_{sample} in Bq) and ^{13}C incorporation ($\delta^{13}\text{C}_M$ in ‰) of sampled
 644 corals are also shown. Values of ^{45}Ca activity and $\delta^{13}\text{C}$ are mean \pm standard error of the mean (SE) associated with the measurement of
 645 three aliquots for each coral.

Experiment	Beaker#	ΔA_T	SE ΔA_T	$\Delta[Ca^{2+}]$	SE $\Delta[Ca^{2+}]$	Activity _{sample}	SE Activity _{sample}	$\delta^{13}\text{C}_M$	SE $\delta^{13}\text{C}_M$
Ambient pH - ^{45}Ca - Light	1	-343.6	1.3	-166.0	6.0	78.5	1.9	-	-
	2	-368.9	0.9	-174.1	5.1	86.5	2.9	-	-
	3	-336.9	0.9	-181.3	2.7	78.2	2.3	-	-
	4	-364.3	0.9	-190.6	6.3	85.2	0.8	-	-
	5	-406.7	0.7	-225.6	1.4	95.7	2.6	-	-
	6	-407.5	1.2	-175.9	1.1	100.6	3.5	-	-
Ambient pH - ^{13}C - Light	1	-386.3	1.5	-195.0	3.8	-	-	-1.4	2.0
	2	-422.6	1.3	-206.8	4.2	-	-	1.8	3.2



3	-405.4	1.9	-200.9	2.1	-	-	3.4	5.1
4	-481.6	1.3	-253.2	2.0	-	-	1.1	2.0
5	-498.4	1.3	-260.5	5.7	-	-	0.8	0.7
6	-618.1	1.8	-317.7	4.4	-	-	0.1	1.8
1	-300.5	1.4	-168.9	0.6	-	-	-0.3	1.3
2	-440.8	1.4	-220.7	2.5	-	-	-3.0	0.5
3	-223.5	1.9	-135.1	0.8	-	-	-3.1	0.6
4	-347.3	1.1	-185.3	0.2	-	-	0.5	5.4
5	-571.7	1.3	-301.7	1.2	-	-	0.6	2.1
6	-434.5	1.3	-224.6	3.7	-	-	0.7	6.1
1	-290.2	1.6	-157.9	2.2	56.44	1.24	-	-
2	-274.3	1.2	-130.4	4.4	50.1	0.74	-	-
3	-300.8	1.3	-168.3	0.9	57.17	1.75	-	-
4	-327.0	2.7	-139.3	5.3	66.24	0.69	-	-
5	-342.8	1.2	-172.6	3.0	68.37	3.11	-	-
6	-228.3	1.8	-113.4	2.5	52.36	2.49	-	-



Lowered pH - ⁴⁵ Ca - Light	1	-59.3	2.2	-1.6*	6.9	20.2	0.7	-
	2	-44.2	2.2	-11.0	2.2	15.3	0.4	-
	3	-71.3	2.8	-28.0	5.9	22.5	0.3	-
	4	-70.2	2.4	-35.7	7.6	23.4	0.4	-
	5	-56.4	2.5	-19.6	7.1	20	0.9	-
Lowered pH - ⁴⁵ Ca - Dark	1	-745.6*	13.2	0.8*	0.3	14.5	0.2	-
	2	-52.4	2.1	-1.0*	1.0	22.1	0.3	-
	3	-50.5	2.1	-22.5	2.8	22.1	0.1	-
	4	-54.3	2.1	-30.3	8.5	23.3	0.4	-
	5	-99.4	2.1	-32.8	4.1	16.1	0.1	-



647 Table 4. Model-II regression results of the comparison between calcification rates estimated
 648 using the different methods considered in this study: the alkalinity and calcium anomaly
 649 techniques (G_{AT} and G_{Ca} , respectively) as well as the ^{45}Ca and ^{13}C incorporation techniques
 650 (G_{45Ca} and G_{13C} , respectively). The number of samples (n), the regression coefficient (R^2), as
 651 well as the slope and intercept (including their 95% confidence intervals, 95% CI) are shown
 652 for each comparison. Few identified outliers ($n = 4$) have been removed from the analyses,
 653 see Table 3 and Table A1.

Methods compared	n	R^2	Slope				Intercept	
			Value		95% CI		Value	95% CI
			Low	High	Low	High	Low	High
G_{AT} vs. G_{Ca}	32	0.98	0.95	0.90	1.00	0.09	0.00	0.18
G_{AT} vs. G_{45Ca}	21	0.99	0.94	0.90	0.98	0.09	0.03	0.15
G_{Ca} vs. G_{45Ca}	20	0.97	1.00	0.91	1.09	-0.06	-0.20	0.07
G_{AT} vs. G_{13C}	12	0.33	0.49	0.05	1.2	0.77	-1.2	2.1
G_{Ca} vs. G_{13C}	12	0.32	0.46	0.03	1.1	0.94	-0.9	2.2

654



655 Table 5. Incubation times (t_{\min} ; h) necessary to obtain significant signals using the three
 656 methods: the alkalinity anomaly technique (A_T), the calcium anomaly technique (Ca^{2+}) and
 657 the ^{45}Ca incorporation techniques (^{45}Ca), see text for calculation procedures. t_{\max} (h) is the
 658 maximum incubation time to maintain carbonate chemistry within an acceptable range ($\Delta C_T <$
 659 10%). The ratios between incubation volume (in mL) and the size of the nubbins (in cm),
 660 considered in our study for the different sets of incubations (Ambient pH vs Low pH; Light vs
 661 Dark), are also shown. t_{\min} values are noted in bold when higher than t_{\max} .

	Ratio V:S	t_{\min} (h)			t_{\max} (h)
		A_T	Ca^{2+}	^{45}Ca	
Ambient pH – Light	77-95	0.26	1.00	0.6	49.7
Ambient pH – Dark	59-69	0.33	2.10	1.5	12.1
Lowered pH – Light	109-121	1.25	6.15	1.1	2.8
Lowered pH – Dark	95-109	1.60	11.20	3.4	4.4

662



663 Table A1. Calcification rates estimated by the different methods considered in this study: the alkalinity and calcium anomaly techniques
 664 (G_{AT} and G_{Ca} , respectively) as well as the ^{45}Ca and ^{13}C incorporation techniques (G_{45Ca} and G_{13C} , respectively). All rates are mean \pm
 665 standard errors of the mean (SE) and are expressed in $\mu\text{mol CaCO}_3 \text{ g DW}^{-1} \text{ h}^{-1}$.

Experiment	Beaker#	G_{AT}	SE G_{AT}	G_{Ca}	SE G_{Ca}	G_{45Ca}	SE G_{45Ca}	G_{13C}	SE G_{13C}
Ambient pH - ^{45}Ca - Light	1	3.28	0.01	3.17	0.11	3.41	0.08	NA	NA
	2	3.21	0.01	3.03	0.09	3.29	0.11	NA	NA
	3	2.69	0.01	2.89	0.04	2.77	0.08	NA	NA
	4	3.38	0.01	3.54	0.12	3.48	0.03	NA	NA
	5	2.41	0.00	2.68	0.02	2.53	0.07	NA	NA
	6	2.43	0.01	2.10	0.01	2.65	0.09	NA	NA
Ambient pH - ^{13}C - Light	1	3.26	0.01	3.29	0.06	NA	NA	1.92	1.35



Ambient pH - ¹³ C - Dark										
2	3.30	0.01	3.23	0.07	NA	NA	4.27	2.27		
3	3.09	0.01	3.06	0.03	NA	NA	5.47	3.66		
4	2.98	0.01	3.14	0.02	NA	NA	3.74	1.36		
5	2.80	0.01	2.92	0.06	NA	NA	3.49	0.41		
6	2.73	0.01	2.81	0.04	NA	NA	3.00	1.22		
1	1.33	0.01	1.50	0.01	NA	NA	2.58	0.79		
2	1.63	0.01	1.63	0.02	NA	NA	0.68	0.23		
3	0.85	0.01	1.03	0.01	NA	NA	0.61	0.30		
4	1.24	0.00	1.32	0.00	NA	NA	3.14	3.67		
5	1.96	0.00	2.07	0.01	NA	NA	3.21	1.35		
6	1.42	0.00	1.46	0.02	NA	NA	3.28	4.16		



Ambient pH - ⁴⁵ Ca - Dark	1	1.59	0.01	1.72	0.02	1.54	0.03	NA	NA
	2	1.39	0.01	1.32	0.04	1.26	0.02	NA	NA
	3	1.46	0.01	1.64	0.01	1.43	0.04	NA	NA
	4	1.29	0.01	1.10	0.04	1.33	0.01	NA	NA
	5	1.44	0.01	1.45	0.03	1.44	0.07	NA	NA
	6	0.75	0.01	0.75	0.02	0.89	0.04	NA	NA
Lowered pH - ⁴⁵ Ca - Light	1	1.00	0.04	0.05*	0.23	0.85	0.03	NA	NA
	2	0.66	0.03	0.33	0.07	0.58	0.02	NA	NA
	3	0.96	0.04	0.75	0.16	0.80	0.01	NA	NA
	4	1.04	0.04	1.06	0.23	0.94	0.02	NA	NA
	5	0.75	0.03	0.52	0.19	0.73	0.03	NA	NA



Lowered pH - ⁴⁵ Ca - Dark	1	2	3	4	5										
	4.05*	0.22	0.25	0.30	0.48	0.07	0.01	0.01	0.01	0.01	0.01	0.01	0.01	0.01	0.01
	-0.01*	0.01*	0.22	0.34	0.32	0.00	0.01	0.03	0.10	0.04	0.04	0.04	0.04	0.04	0.04
	0.20	0.24	0.30	0.35	0.21	0.00	0.00	0.00	0.01	0.00	0.00	0.00	0.00	0.00	0.00
	NA	NA	NA	NA	NA	NA	NA	NA	NA	NA	NA	NA	NA	NA	NA



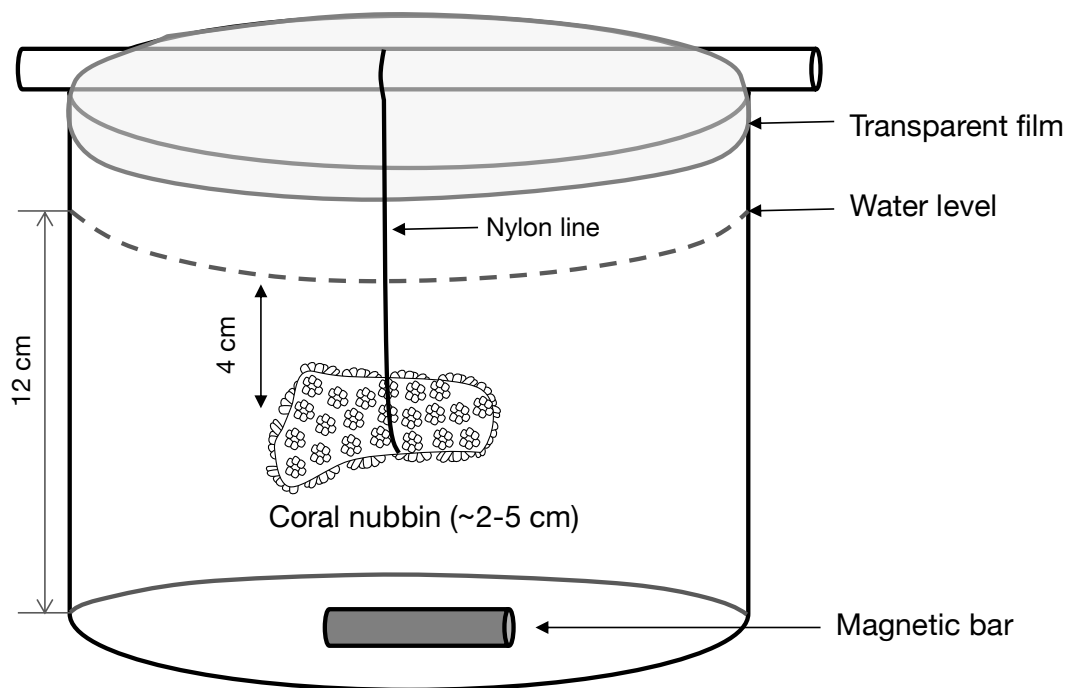
667 **Figure captions**

668 Fig. 1. Scheme of the polyethylene container in which a coral nubbin is suspended with a
669 nylon line and covered with a transparent film.

670 Fig. 2. Calcification rates estimated based on the alkalinity anomaly technique (G_{AT}) as a
671 function of calcification rates estimated based on the calcium anomaly technique (G_{Ca}). The
672 dashed line represents the 1:1 relationship while the full line represents the model-II
673 regression relationship. Horizontal error bars represent standard errors (SE) associated with
674 the estimation of G_{Ca} . Vertical error bars representing SE associated with the estimation of
675 G_{AT} are too small to be visible. The corresponding dataset can be found in Table A1.

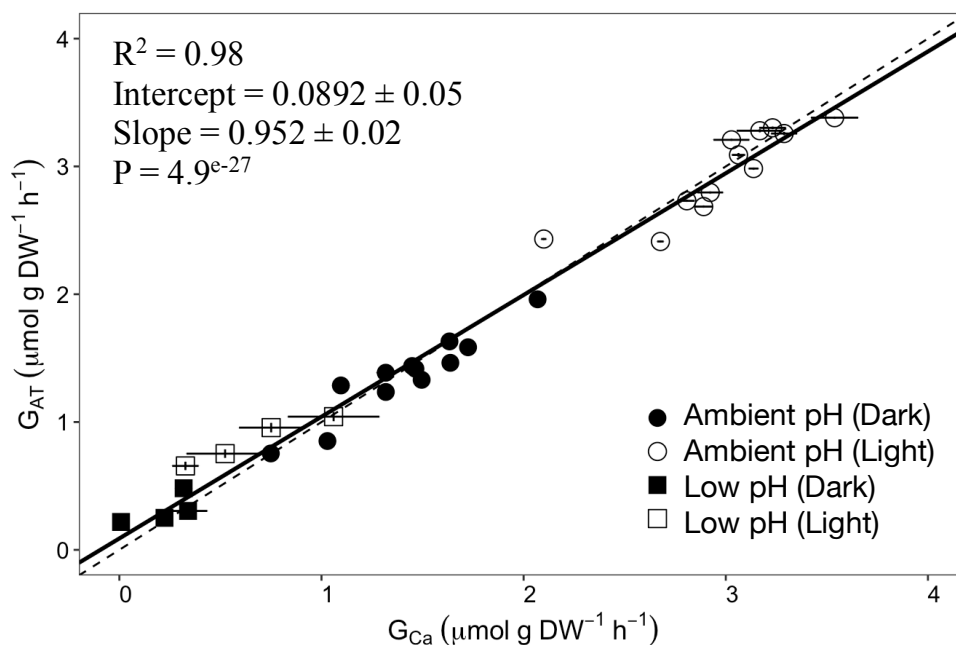
676 Fig. 3. Calcification rates estimated based on the alkalinity anomaly technique (G_{AT}) as a
677 function of calcification rates estimated based on the ^{45}Ca incorporation technique ($G_{45\text{Ca}}$).
678 The dashed line represents the 1:1 relationship while the full line represents the model-II
679 regression relationship. Horizontal error bars represent standard errors (SE) associated with
680 the estimation of $G_{45\text{Ca}}$. Vertical error bars representing SE associated with the estimation of
681 G_{AT} are too small to be visible. The corresponding dataset can be found in Table A1.

682 Fig. 4. Calcification rates estimated based on the alkalinity anomaly technique (G_{AT}) as a
683 function of calcification rates estimated based on ^{13}C incorporation technique ($G_{13\text{C}}$). The
684 dashed line represents the 1:1 relationship while the full line represents the model-II
685 regression relationship. Horizontal error bars represent standard errors (SE) associated with
686 the estimation of $G_{13\text{C}}$. Vertical error bars representing SE associated with the estimation of
687 G_{AT} are too small to be visible. The corresponding dataset can be found in Table A1.



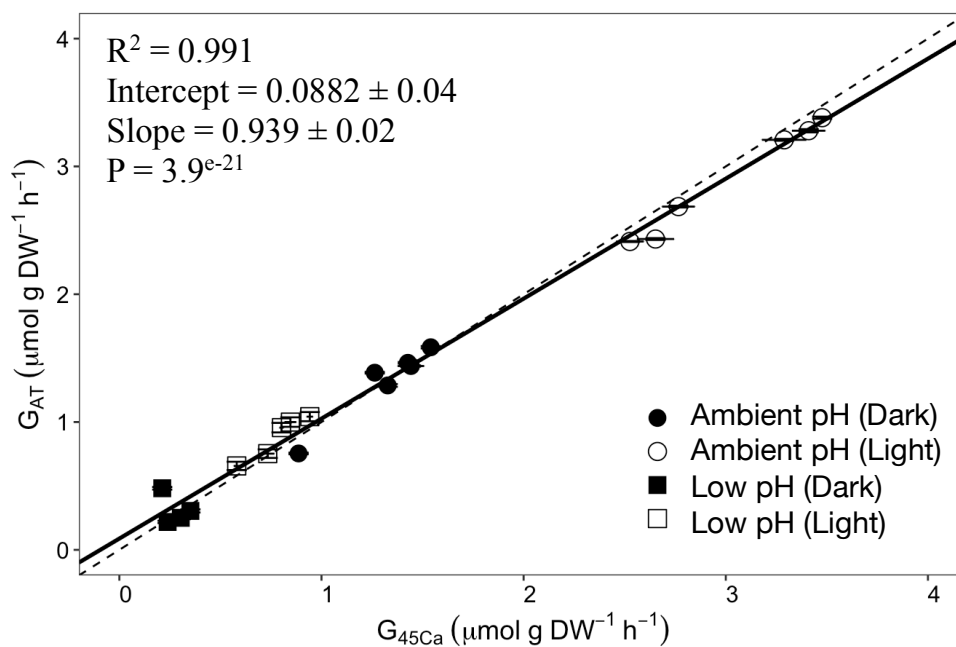
688

689 Fig. 1.



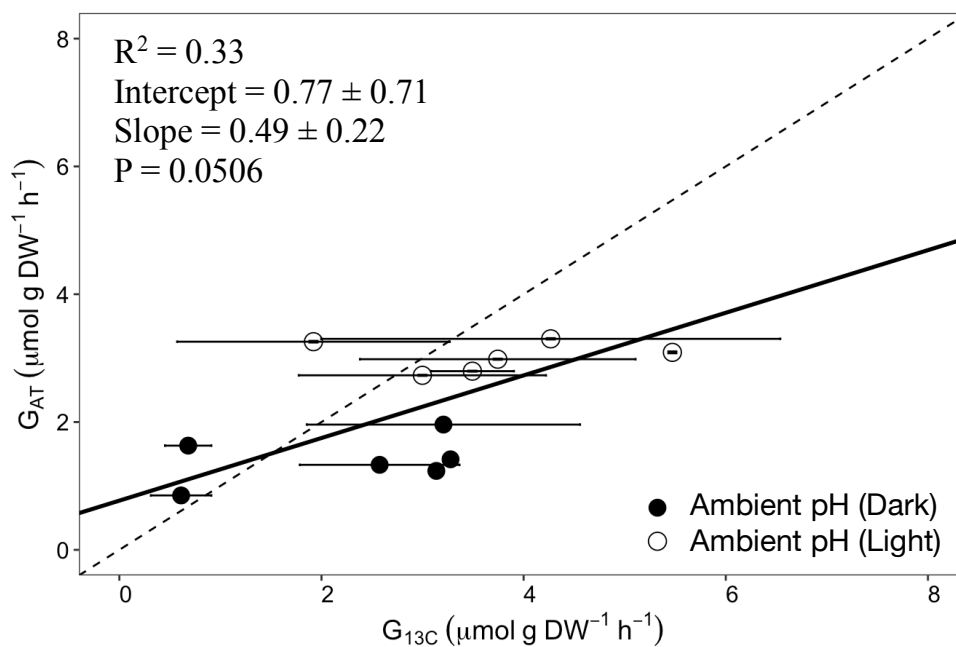
690

691 Fig. 2.



692

693 Fig. 3.



694

695 Fig. 4.